Journal of the Korean Astronomical Society
51: 73 ∼ 88, 2018 June

http://dx.doi.org/10.5303/JKAS.2018.51.4.73
pISSN: 1225-4614 · eISSN: 2288-890X
http://jkas.kas.org

Luminosity Profiles of Prominent Stellar Halos

Hong Bae Ann and Hyeong Wook Park
Pusan National University, 2 Busandaehak-ro, Geumjeong-gu, Busan 46241, Korea; hbann@pusan.ac.kr

Received May 9, 2018; accepted June 30, 2018

Abstract: We present a sample of 54 disk galaxies which have well developed extraplanar structures. We selected them using visual inspections from the color images of the Sloan Digital Sky Survey. Since the sizes of the extraplanar structures are comparable to the disks, they are considered as prominent stellar halos rather than large bulges. A single Sérsic profile fitted to the surface brightness along the minor-axis of the disk shows a luminosity excess in the central regions for the majority of sample galaxies. This central excess is considered to be caused by the central bulge component. The mean Sérsic index of the single component model is 1.1 ± 0.9. A double Sérsic profile model that employs $n = 1$ for the inner region, and varying n for the outer region, provides a better fit than the single Sérsic profile model. For a small fraction of galaxies, a Sérsic profile fitted with $n = 4$ for the inner region gives similar results. There is a weak tendency of increasing n with increasing luminosity and central velocity dispersion, but there is no dependence on the local background density.

Key words: galaxies: general — galaxies: photometry — galaxies: structure

1. Introduction

Stellar halos are thought to be ubiquitous in disk galaxies (Sackett et al. 1994; Morrison et al. 1997; Lequeux et al. 1998; Abe et al. 1999; Zibetti et al. 2004; Zibetti & Ferguson 2004; Zibetti et al. 2004; McConnachie et al. 2006; Chapman et al. 2006; Kalirai et al. 2006; Seth et al. 2007; de Jong et al. 2007; Mouhcine et al. 2007; Helmi 2008; Jablonka et al. 2010; Ibata et al. 2014). In the framework of the Λ cold dark matter (ΛCDM) cosmology (Springel et al. 2006), the existence of stellar halos around disk galaxies is very natural because they are byproducts of hierarchical galaxy formation. They are thought to be formed by the accretion and disruption of dwarf satellites (Bullock & Johnston 2005; Abadi et al. 2006; Font et al. 2006; de Lucia & Helmi 2008; Font et al. 2008; Johnston et al. 2008; Gilbert et al. 2009; Cooper et al. 2010; Zolotov et al. 2010). There is mounting evidence that the accretion and disruption of infalling satellites play a major role in building the stellar halos around disk galaxies (Searl & Zinn 1978; Johnston et al. 1996; Helmi & White 1999; Ferguson et al. 2002; Bullock & Johnston 2005; Ibata et al. 2007; Johnston et al. 2008; Romanowsky et al. 2016). On the other hand, gas rich mergers in the early phase of the galaxy assembly (Brook et al. 2004), and $in-situ$ star formation (Font et al. 2011) were also proposed as explanations of the origin of stellar halos. The ejection of $in-situ$ stars formed at high redshift ($z \gtrsim 3$) by subsequent major (Zolotov et al. 2009) and minor mergers (Purcell et al. 2010) also could contribute to stellar halos.

The surface brightness of the stellar halos of spiral galaxies is typically 10 magnitudes below the night sky background (Bakos & Trujillo 2012), making them difficult to observe. In the case of the Milky way, its halo luminosity is ∼ 1 per cent of the total luminosity, and other spirals usually have halo luminosities similar to the Milky Way (Courteau et al. 2011). Since the surface brightness level needed to analyze the structure of stellar halos is so faint (∼ 30 mag arcsec^{-2}), it requires highly precise observations and data reductions are required to prevent observational artifacts. The first detection of the stellar halo around disk galaxies was reported for NGC5907 by Sackett et al. (1994), and confirmed by Lequeux et al. (1996) and Lequeux et al. (1998). Zibetti et al. (2004) applied an image stacking technique to disk galaxies to derive the structural parameters of their stellar halos. They showed that stellar halos are moderately flattened spheroids with spatial luminosity distributions that are well described by a power law ($\sim r^{-3}$).

On the other hand, there are some disk galaxies with prominent stellar halos which are bright enough to be visually identified. A well known example is NGC 4594 (M104), a spiral galaxy, known as the Sombrero galaxy, with a Hubbe type of Sa (de Vaucouleurs et al. 1991) however, it is sometimes considered as a peculiar elliptical galaxy (McQuinn et al. 2016) because of its bright stellar halo. The nucleus of NGC 4594 is fairly bright, and there is a supermassive black hole in the center (Kormendy 1988, 1996; Ho et al. 1997). More often, the prominent stellar halo of NGC 4594 is considered as a massive bulge which contains ∼ 90% of the total luminosity (Kent 1988). However, the $V-$band minor axis profile of NGC 4594 (Jarvis & Freeman 1985) shows a break at ∼ 55 arcsec which suggests two components, a stellar halo and central bulge. Detailed surface photometry of NGC 4594 (Burkhead 1986) also showed that the outer spheroidal component is a prominent stellar halo that can be well approximated by an ellipsoid with an

Corresponding author: H. B. Ann

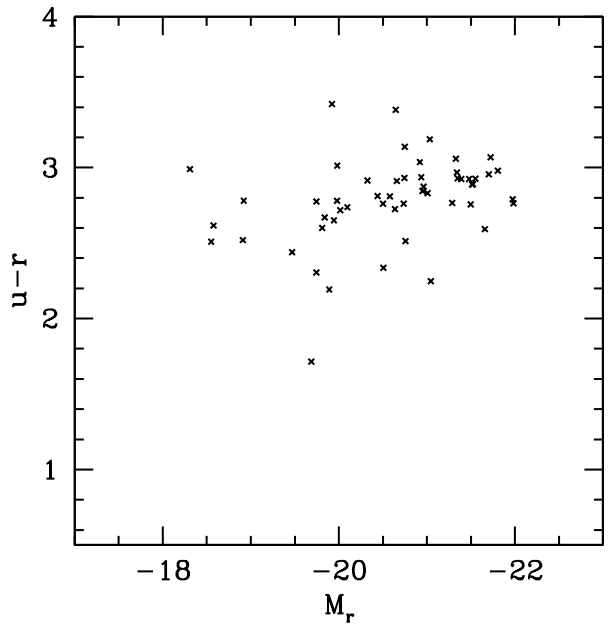

Figure 1. Color-magnitude diagram of the sample galaxies that show prominent stellar halos.

axis ratio of $b/a = 0.64$. A clear distinction between the central bulge and the stellar halo can be seen in the Spitzer 3.6-μ image (Gadotti & Sánchez-Janssem 2012), in which the stellar halo is rounder than the central bulge, and dominates over the disk and bulge at large radius ($r \gtrsim 215$ arcsec).

Since most stellar halos are too faint to be observed by conventional methods, the number of galaxies with detailed observations of their stellar halos is quite limited. Therefore, there are no statistical samples of the structure and physical properties of stellar halos. On the other hand, stellar halos have been well predicted by numerical simulations (Katz & Gunn 1991; Steinmetz & Muller 1995; Brook et al. 2004) in the CDM scenario (White & Frenk 1991; Kauffmann et al. 1993). In a sense, these simulations failed to reproduce Milky Way type stellar halos whose mass fraction is less than ~ 1 per cent of the total luminous matter. Most stellar halos that they modeled were too massive compared to observed stellar halos. However, Brook et al. (2004) was able to make different kinds of stellar halos depending on the supernova (SN) feedback mechanisms used. One model is similar to the faint stellar halos, often observed, and another is similar to the massive stellar halos that were reported in the previous studies (Katz & Gunn 1991; Steinmetz & Muller 1995). Although prominent stellar halos can easily be observed by conventional methods, there is no extensive study of the prominent stellar halos due to their rarity in the local universe. Observations of prominent stellar halos, however, seem to be a promising path to understanding the structural properties of stellar halos. This study will uncover a wealth of information about the formation and evolution of galaxies.

The purpose of this study is to construct a sample of prominent stellar halos and establish basic statistics. In particular, we aim to derive the Sérsic index of the luminosity profile of the prominent stellar halos to characterize the shape of the luminosity distribution. The Sérsic index n is known to be correlated with the luminosity, effective radius, and the central velocity dispersion of galaxies (Graham et al. 2001; Mollenhoff & Heidt 2001; Graham 2002) when applied to ellipticals and the bulges of disk galaxies, Since prominent stellar halos are rare phenomena, we are also interested in their environment.

This paper is organized as follows. The data and sample selection are described in Section 2, and the results of the present study are given in Section 3. Discussion and conclusions are provided in Section 4.

2. DATA AND SAMPLE SELECTION

2.1. Selection of Prominent Stellar Halos

We selected prominent stellar halos using the color images provided by the Sloan Digital Sky Survey (SDSS) Data Release 7 (Abazajian et al. 2009). We used the Korea Institute of Advanced Study Value-Added Galaxy Catalog (KIAS-VAGC; Choi et al. 2010) to select the parent sample of target galaxies that have redshifts less than $z = 0.032$, and r-magnitudes brighter than 17.77. The number of parent sample galaxies is 44,244. We first selected 7,810 edge-on galaxies through visual inspections of the SDSS color images in the parent sample. Because of the large axis ratios (b/a) of the prominent stellar halos, they are likely to be omitted in the sample of edge-on galaxies selected by axis ratio criteria. Thus, it is necessary to conduct a visual inspection of the color images to see whether or not galaxies are edge-on. The selection criterion we have applied is the axis ratio of the disks and not the entire galaxy. Sometimes, a well distinguished dustlane is considered as evidence of edge-on disks.

Since we have selected the prominent stellar halos by visual inspections of the color images without quantitative selection criteria, the selected sample is subject to some personal bias, but we do not think we omit a significant fraction of prominent stellar halos. The final sample contains 54 galaxies, and corresponds to 0.1% of the parent sample of 44,244 galaxies, and 0.7% of the 7810 edge-on galaxies. This means that prominent stellar halos are very rare. The basic properties of the 54 galaxies are presented in Table 1, most of which are obtained from the KIAS-VAGC.

Figure 1 shows the color-magnitude diagram of galaxies in the final sample. M_r is derived from the $r-$band model magnitude corrected for Galactic extinction using the $r-$band extinction values from SDSS DR7. A K-correction and an evolution correction are not applied. Distances to the galaxies were derived from the redshifts, corrected for the motion relative to the centroid of the local Group (Mould et al. 2000). For galaxies with $z < 0.01$, the metric distances provided by NED are used. The galaxies lying inside a 10°-cone around M87 with redshift less than $z = 0.007$ are assumed to be the members of the Virgo Cluster, and the

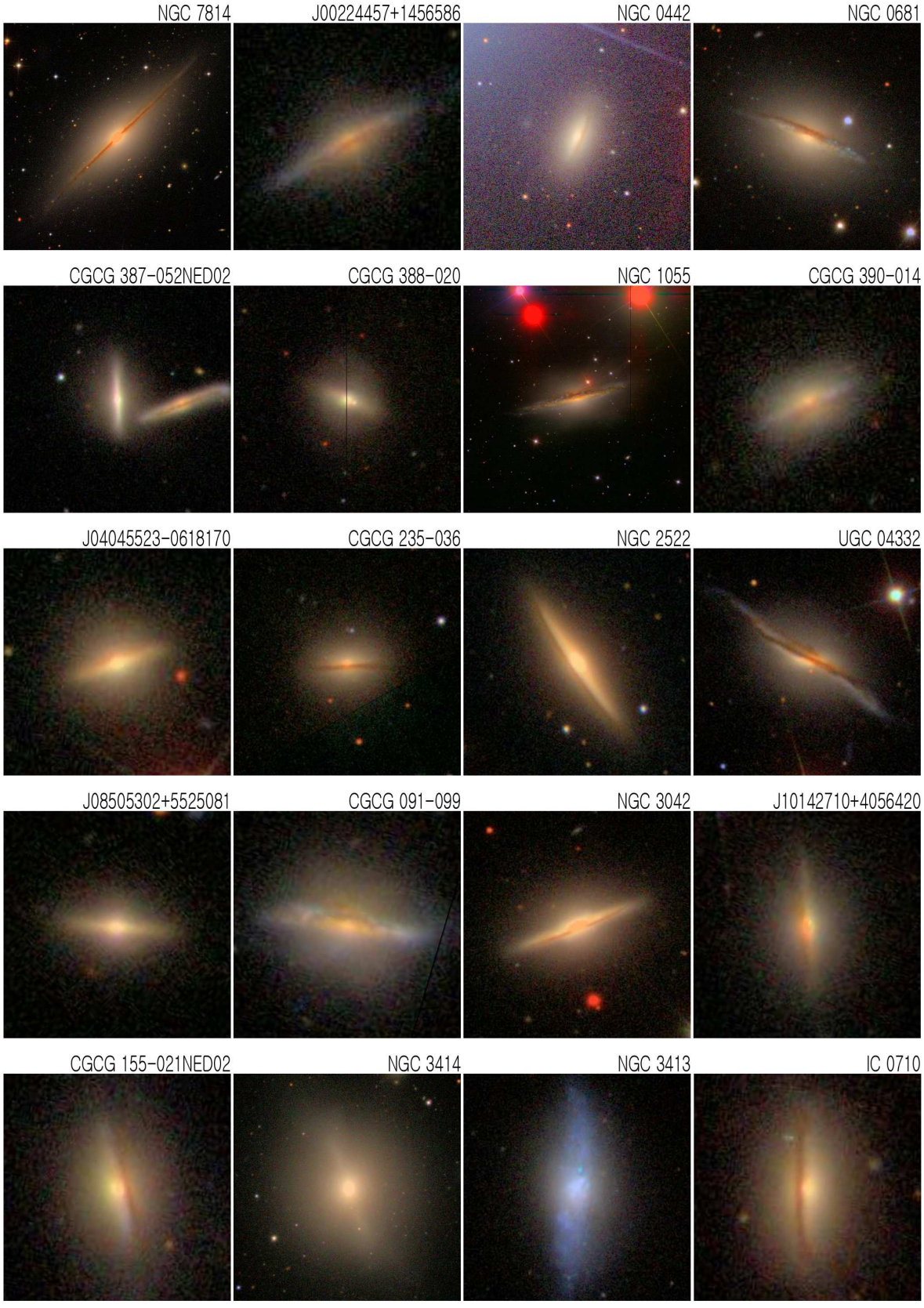

Figure 2. Images of disk galaxies that show prominent stellar halos. The image sizes are adjusted to fit to the frame size.

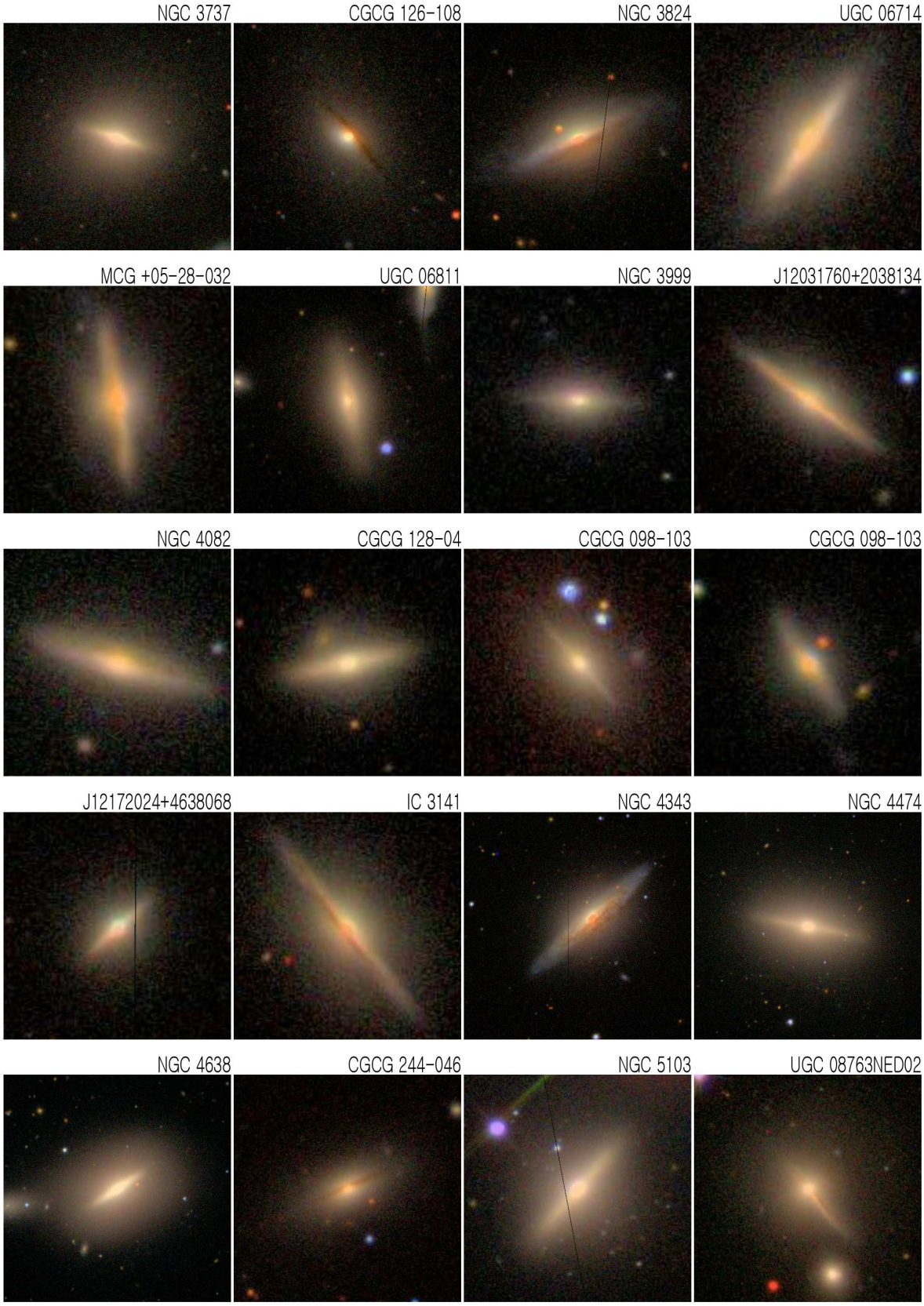

Figure 2. *Continued.*

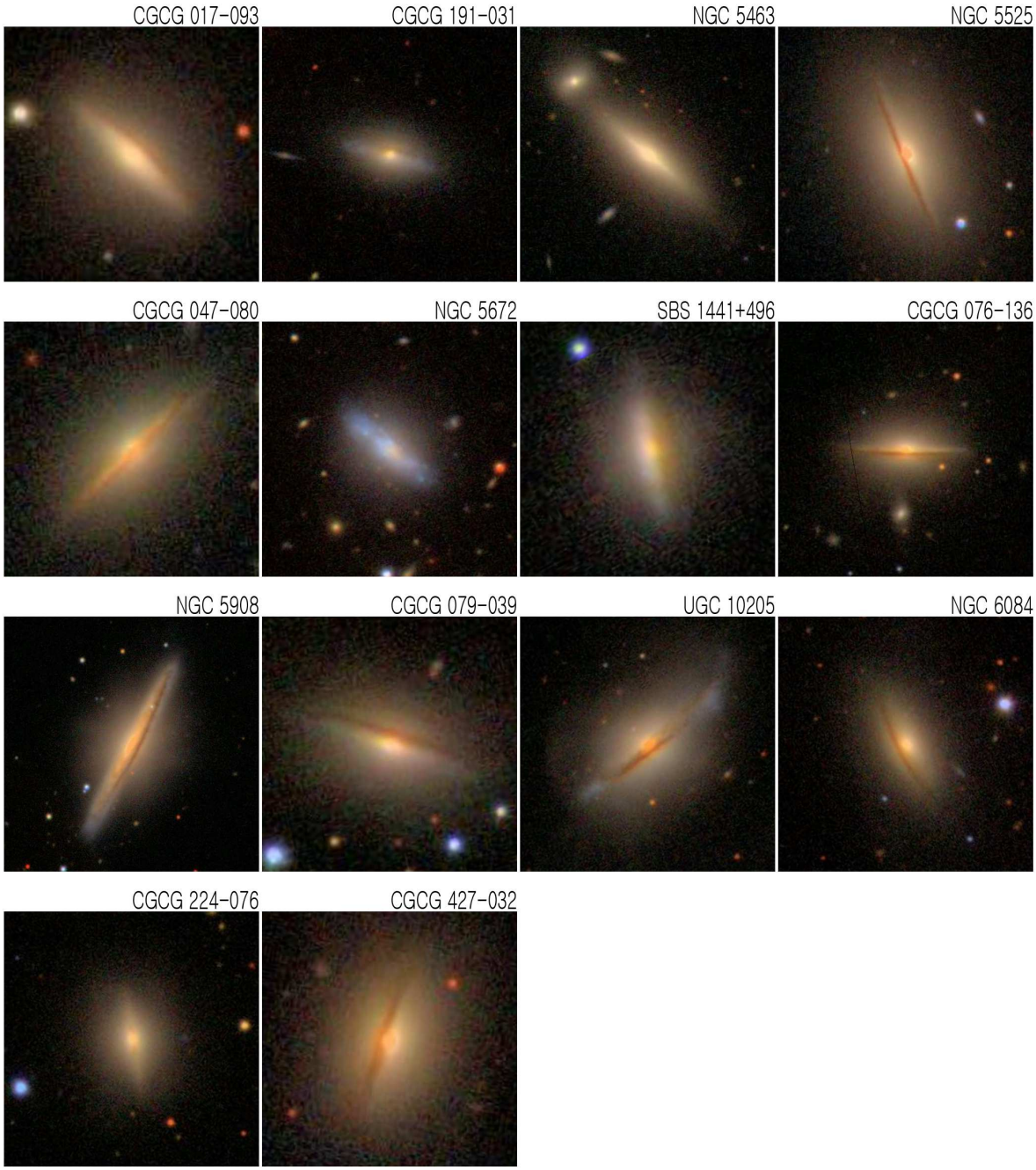

Figure 2. *Continued.*

distance of the Virgo cluster is used for those galaxies. We assumed the Virgo distance as $D = 16.7$ Mpc and H=75 km s^{-1} Mpc^{-1}. It is evident that the galaxies with prominent stellar halos have photometric properties similar to the galaxies in the red sequence defined by early type galaxies, particularly by elliptical galaxies.

3. RESULTS

3.1. Morphological Properties of Prominent Stellar Halos

Figure 2 shows the color images of the 54 sample galaxies from the SDSS DR7. At first glance, the prominent stellar halos are mostly flattened ellipsoids. They have somewhat red colors, typical of old stellar popula-

tions, and sizes comparable to their disks. Some halos have sizes about half that of their disk, while some halos are nearly spherical. For the majority of sample galaxies dust lanes can be observed, some of which are offset from the central bulge, and middle plane of the disk. One of the remarkable morphological properties of galaxies with prominent stellar halos is that they are early type disk galaxies, mostly S0 and S0/a galaxies, without well developed bulges. Most of the luminosity around the disk come from the stellar halo, and not from the bulge. The bulge luminosity is confined to the central regions. Of course, as shown in previous studies (Hes & Peletier 1993), the prominent structures around the disk plane can be considered as an extended bulge. However, as will be shown below, the extraplanar prominent structures are considered here as stellar halos.

As can be seen in Figure 2, most galaxies with prominent stellar halos have red disks except for the two extremely blue disks (NGC 3413 and NGC 5672) and show well distinguished dustlanes. There are several galaxies whose disk morphology differs from that of others. They have disks with somewhat blue colors in the outer parts, indicating spiral arms (2MASX J00224457+1456586, UGC04332, CGCG 091-099, NGC 4343, CGCG 191-031, UGC 10205). Warped disks are observed in a small fraction of sample galaxies.

Figure 3 shows the histogram of the axial ratios (b/a) of the sample galaxies along with the axial ratios of a sample of elliptical galaxies in the local universe ($z \lesssim 0.01$) from the catalog of Ann et al. (2015). The axis ratios of the sample galaxies were taken from the KIAS-VAGC (Choi et al. 2010) where the major- and minor-axis length were derived from the i-band isophotal maps. the two types of galaxies in the local universe show a similar distribution of axis ratios. Since the lengths of the major axis of the stellar halos and the disks are similar, the axial ratios of the sample galaxies are determined by the shape of the halos. Thus, the similarity between the two axis ratio distributions suggests that the prominent stellar halos are flattened ellipsoids, similar to the elliptical galaxies.

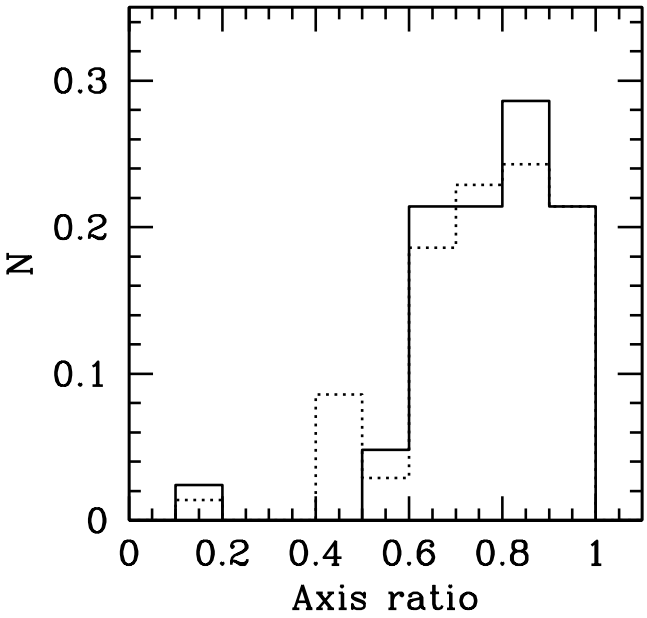

Figure 3. Frequency distribution of axis ratios of the disk galaxies which have prominent stellar halos, compared to elliptical galaxies in the local universe ($z \lesssim 0.01$). Solid lines represent the galaxies with prominent stellar halos and dotted lines indicate the local elliptical galaxies.

3.2. Luminosity Profiles of the Prominent Stellar Halos

Surface photometry of the r-band images for the sample galaxies is used to derive the luminosity profiles of the prominent stellar halos. We used the mode of pixel values around the target galaxy as the sky background, I_{sky}, to derive the galaxy intensity distribution given by $I_g = I_{obs}(x, y) - I_{sky}$. We used the SPIRAL (Ichikawa et al. 1987; Okamura 1988) to extract the surface brightness profiles along the minor-axis, where the luminosity of the stellar halo is less affected by the disk luminosity. The effect of dustlanes is also negligible in the minor-axis profiles, especially in the halo regions.

The bulge and halo are the main contributors to the luminosity profile along the minor-axis. In most normal disk galaxies the contribution of halo component is negligibly small compared to that of the bulge. But, in the case of disk galaxies with prominent stellar halos, the luminosity of the stellar halo is larger than that of the bulge. In particular, the luminosity distribution at radii larger than a few times the effective radius of the bulge is dominated by the stellar halo. The surface brightness profiles along the minor-axis of the sample galaxies are examined to see whether the sample galaxies have two components. Breaks in the surface brightness profiles are considered as the signature of multiple components. The majority of the sample galaxies are found to have a break at $r \lesssim 10$ arcsec from the center, indicating the existence of a central bulge.

Several functional forms are commonly used to represent the luminosity profiles of galaxies. In the early era of galaxy studies, the Hubble profile, $I(r) = I_0/(1 + (r/r_c)^2)$, was employed to represent the luminosity distribution of elliptical galaxies. Later, de Vaucouleurs (1958) introduced the $r^{1/4}$-law to represent the luminosity distributions of the bulge of spiral galaxies as well as the elliptical galaxies. Freeman (1970) introduced exponential function to describe the luminosity distribution of the disks of spiral galaxies. These functions have been used very successfully to describe the luminosity distributions of ellipticals and spirals. Sérsic (1968) introduced a generalized function to represent luminosity distribution of galaxies including both ellipticals and spirals. The Sérsic function is defined by three parameters, I_{eff}, r_{eff}, and n as follows

$$I(r) = I_{eff} exp(-b_n((r/r_{eff})^{1/n} - 1)$$

where r_{eff} and I_{eff} are the effective radius and effective intensity (which is the intensity at $r = r_{eff}$), respectively. The parameter n is the Sérsic index. The

constant b_n is approximated by $b_n = 1.9992n - 0.3271$ (Caon et al. 1993; Prugniel & Simen 1997). The de Vaucouleurs law and exponential law are the cases for $n = 4$ and $n = 1$, respectively.

As there is no commonly used functional form for the luminosity profile of prominent stellar halos, both the Hubble profile and the Sérsic profile are examined to determine which is more representative of the luminosity distribution. The Hubble profile is known to represent the luminosity distribution of the stellar halos of edge-on galaxies obtained by image stacking techniques (Zibetti et al. 2004), However, it was found that the Hubble profile does not fit well to the observed luminosity distributions of the majority of the sample galaxies in our sample. On the contrary, the Sérsic profile better represents the luminosity distribution of the prominent stellar halos.

Figure 4 shows the results of fitting a single Sérsic profile along the minor-axis. A χ^2 minimization technique is applied to derive the three free parameters, n, r_{eff} and I_{eff}, with fitting ranges selected from the visual inspection of the minor-axis profiles. The bulge dominated regions are avoided during fitting a single Sérsic profile to the observed profiles. The resulting profiles are insensitive to the fitting ranges except in the far outer regions where the surface brightness is affected by the background sky or by other components such as rings. For some galaxies, there are wiggles or bumps at large radii which are due to the contamination from nearby objects or in the case of large bumps due to outer rings or shell structures.

At first glance, the observed luminosity distributions of prominent stellar halos are well represented by the Sérsic profiles. As shown in Figure 5, the fitted Sérsic index n varies from 0.5 to 3.5 with a peak near $n = 1.2$. About 90% of the sample galaxies have n less than 3. For the majority of galaxies. there is a luminosity excess over the halo profile at small radii. This central luminosity excess is mostly due to the bulge which is not taken into account in the profile fittings. There are 46 galaxies in the sample(85%) that show a clear luminosity excess. Since the luminosity excess is due to the luminosity of the bulge, the luminous structures around the disk plane must be stellar halos. Thus, this study presents a statistically significant sample of the structures of stellar halos for the first time. The stellar halos are prominent enough to be visually identified from conventional images, such as SDSS. The three parameters of the single component Sérsic profile are listed in Table 2.

Since the majority of sample galaxies show a central luminosity excess, which is assumed to be due to bulge component, the luminosity distributions along the minor-axis of sample galaxies are also fitted by two Sérsic functions, one for the bulge and the other for the halo. The iterative fitting technique (Kormendy 1977) is applied to decompose the bulge and halo simultaneously. The iterative profile decomposition technique assumes fitting ranges for each component where one component dominates the other. A small change in the bulge fitting range affects the decomposition significantly. Thus, the bulge fitting range is selected interactively by minimizing the residuals of the fit. At first, $n = 4$, (i.e., de Vaucouleurs law), was assumed for the bulge, and n was varied for the halo. Using these parameters the fittings were unsuccessful for the majority of the sample galaxies. Various alternative values of n were explored for the bulge, and the Sérsic index of $n \approx 1$ is found to well represent most galaxies. Since $n = 1$ gives successful fits for most of the sample galaxies, $n = 1$ is used as the default Sérsic index for the bulge component. However, n=4 was adopted if $n = 4$ gives a similar result. In general, the Sérsic index of the stellar halo in the two component model becomes smaller than that of the single component model. The Sérsic index of the two component models n_b (bulge) and n_h (halo) are listed in Table 2.

It is interesting to note that about 15% of the sample galaxies have shell structures outside of the visible stellar halo. The presence of the shell structure is indicated by the large bump in the minor-axis profiles. The galaxies with well developed outer shell structure are NGC 0442, CGCG 387-052NED0, NGC 3999, NGC 4082, CGCG 098-103, CGCG 244-046, NGC 5463, 2MASX J14443669+1631314, CGCG 076-136.

3.3. Distribution of the Sérsic Index

Figure 5 shows the frequency distribution of the Sérsic index for the 54 stellar halos derived by fitting a single Sérsic function to the surface brightness profiles along the minor-axis of the sample galaxies. Since the detailed shape of the frequency distribution depends on the bin size, due to the small sample size, the frequency distributions using different bin sizes were examined. It was found that the bin size of $\Delta n = 0.3$ is optimum choice for the present sample. It keeps the general shape of the frequency distribution, while suppressing the statistical noise.

It appears that there are at least two peaks, one peak at $n \approx 1.2$, and the other at $n \approx 3.4$. The number of galaxies around the first peak at $n \approx 1.2$ is 37 and it comprises $\sim$ 70% of the total sample. The number of galaxies near the second peak at $n \approx 3.4$ is 4, which is less than 10% of the total sample. The remaining galaxies, comprising the remaining quarter of the total sample, are located near a third peak at $n \approx 2$. Since it is not clear whether the third peak at $n \approx 2$ is a real feature, the sample galaxies are divided into two groups. One group is comprised of the galaxies around the first peak at $n \approx 1.2$, including the galaxies near the third peak at $n \approx 2$, and the other group consists of galaxies around the second peak at $n \approx 3.4$.

The number of galaxies in the larger group is 50 which comprises 93% of the total sample. The mean Sérsic index of this group is 1.42 ± 0.55. If we exclude the galaxies near the third peak at $n \approx 2$, it becomes 1.19 ± 0.35, thus very close to the exponential profile. The distribution of the Sérsic index of this group is similar to that of the dwarf elliptical/spheroidal galaxies (Binggeli & Jerjen 1998; Ryden et al. 1999; Grant et al.

Table 1
Basic properties of 54 disk galaxies with prominent stellar halos.

ID	α_{2000}	δ_{2000}	D[a]	M_r	$u-r$	$g-r$	mc[b]	b/a	σ[c]	Galaxy name[d]
354822	0.812042	16.145420	12.6	-19.92	3.37	1.28	SA(s)ab?	0.25	0.0	NGC 7814
381062	5.685914	14.949751	77.0	-19.89	2.19	0.76	Sa	0.81	98.1	J00224457+1456586
2092266	18.661020	-1.020657	56.4	-21.34	2.97	1.04	S0/a?	0.64	176.4	NGC 0442
323194	27.295120	-10.426420	17.8	-19.98	2.96	1.06	SAB(s)ab	0.68	108.0	NGC 0681
1742502	32.784565	-0.654782	60.3	-20.76	2.51	0.85	Sb	0.70	125.1	CGCG 387-052NED02
809401	37.040436	0.799052	74.7	-21.01	2.83	0.97	S0/a	0.90	193.5	CGCG 388-020
1767358	40.438672	0.442579	10.2	-18.31	1.64	0.88	SBb?	0.52	74.5	NGC 1055
764571	47.772167	-0.546510	84.0	-20.51	2.34	0.78	S0/a	0.74	127.7	CGCG 390-014
326159	61.230087	-6.304820	80.1	-20.96	2.87	0.99	1	0.89	0.0	J04045523-0618170
1728488	116.389717	45.772331	94.8	-21.48	2.92	1.01	S0	0.83	180.6	CGCG 235-036
1905088	121.556000	17.706573	45.8	-21.33	3.06	1.06	S0/a	0.53	273.9	NGC 2522
1875243	124.907845	21.114300	53.7	-20.65	3.38	0.98	S?	0.72	176.1	UGC 04332
225814	132.721054	55.419109	91.6	-20.74	2.76	0.94	S0	0.73	184.5	J08505302+5525081
2257869	142.595779	19.469234	42.4	-19.74	2.31	0.92	2	0.93	71.6	CGCG 091-099
78806	148.334244	0.697720	35.7	-20.93	2.94	1.03	S0	0.70	180.4	NGC 3042
1248278	153.612778	40.945045	68.5	-19.98	3.01	1.11	S0/a	0.68	125.8	J10142710+4056420
1960169	162.291870	29.815895	94.0	-21.35	2.93	1.03	1	0.63	0.0	CGCG 155-021NED02
2204882	162.817932	27.975279	13.9	-19.84	2.85	0.97	S0	0.64	0.0	NGC 3414
1894107	162.836288	32.766331	6.1	-16.07	2.27	0.38	S0	0.57	0.0	NGC 3413
2221022	173.614166	25.876469	93.3	-21.39	2.92	1.04	1	0.63	186.3	IC 0710
965668	173.901520	54.948639	59.0	-21.50	2.76	0.94	SB0	0.77	202.4	NGC 3737
2356878	174.083298	20.521761	63.0	-20.33	2.91	1.02	1	0.72	228.3	CGCG 126-108
873264	175.686890	52.779636	57.6	-20.95	2.84	1.01	SA(s)a?	0.43	146.0	NGC 3824
253847	176.162704	67.955879	28.8	-18.91	2.61	0.92	S?	0.70	74.6	UGC 06714
2205307	177.191284	29.641171	68.4	-20.44	2.81	1.02	2	0.59	0.0	MCG +05-28-032
901271	177.644882	50.529064	69.8	-21.29	2.77	0.93	S0/a	0.58	203.3	UGC 06811
2322850	179.485378	25.068284	41.0	-18.58	2.62	0.88	1	0.69	87.1	NGC 3999
2333089	180.823410	20.636995	61.5	-20.10	2.74	0.95	1	0.60	117.8	J12031760+2038134
1061991	181.297729	10.670613	68.5	-20.66	2.91	1.05	Sbc	0.83	146.0	NGC 4082
2247528	182.475800	25.311249	68.5	-20.50	2.76	0.95	1	0.80	166.9	CGCG 128-04
2414948	183.345688	16.957827	83.9	-20.58	2.81	0.93	1	0.55	185.4	CGCG 098-103
2311827	183.505875	23.010292	72.7	-19.75	2.78	0.96	2	0.77	114.5	J12140140+2300370
1202224	184.334381	46.635284	71.4	-20.02	2.72	0.90	S0/a	0.90	187.7	J12172024+4638068
2319495	184.743393	24.186310	72.8	-20.75	2.93	1.03	2	0.62	200.2	IC 3141
1288874	185.914588	6.951942	9.1	-18.92	3.00	1.02	SA(rs)b?	0.63	101.0	NGC 4343
1828259	187.473083	14.068640	15.2	-19.47	2.63	0.91	S0	0.56	0.0	NGC 4474
959348	190.697632	11.442470	10.9	-19.81	2.80	0.95	S0	0.53	0.0	NGC 4638
1176719	193.205093	47.685013	96.5	-20.92	3.04	1.05	1	0.55	0.0	CGCG 244-046
1227719	200.125336	43.083969	13.7	-18.55	2.71	0.89	S?	0.86	0.0	NGC 5103
1989264	207.772507	25.093710	87.5	-21.97	2.79	0.93	1	0.79	0.0	UGC 08763NED02
49109	208.428314	0.060874	88.4	-21.52	2.89	0.99	S0/a	0.86	221.2	CGCG 017-093
1838833	210.311371	37.882977	74.2	-20.64	2.72	0.95	Sa	0.55	128.5	CGCG 191-031
1340227	211.543945	9.353449	72.2	-21.98	2.76	0.94	S?	0.55	0.0	NGC 5463
2380372	213.913589	14.282601	55.3	-21.51	2.89	0.98	S0	0.67	226.5	NGC 5525
1348148	217.970367	7.320885	81.3	-21.03	3.19	1.12	2	0.69	173.3	CGCG 047-080
1913169	218.159805	31.670155	36.2	-19.69	1.71	0.56	Sb?	0.95	0.0	NGC 5672
980767	220.880341	49.393093	91.1	-21.05	2.25	0.82	Sa	0.83	137.4	SBS 1441+496
1430278	225.568130	11.917582	97.1	-21.81	2.98	1.03	Sa	0.85	203.8	CGCG 076-136
2412381	229.180084	55.409248	34.9	-20.75	3.14	1.11	SA(s)b	0.56	111.9	NGC 5908
1423817	241.207611	8.481091	52.8	-19.94	2.65	0.91	1	0.64	120.3	CGCG 079-039
1393362	241.667435	30.099058	67.1	-21.66	2.59	0.95	Sa	0.58	165.2	UGC 10205
2001255	243.569672	17.757429	91.1	-21.72	3.07	1.07	Sa	0.65	212.5	NGC 6084
532728	249.074478	44.135700	96.0	-21.70	2.95	1.01	S0/a	0.86	220.8	CGC G224-076
726224	328.157928	12.535856	89.1	-21.55	2.93	1.06	E	0.67	222.9	CGCG 427-032

[a] Galaxy distance in unit of Mpc.
[b] Morphological types form the NASA Extragalactic Database. If not available, the KIAS-VAGC morphological class is given: 1 (E/S0) and 2 (Sp/Irr).
[c] Central velocity dispersion in unit of km s^{-1}. In case of no data, we use 0.0.
[d] Galaxy name taken from the NASA Extragalactic Database. We omit '2MASX' for the 2 Micron All Sky Survey Extended objects names.

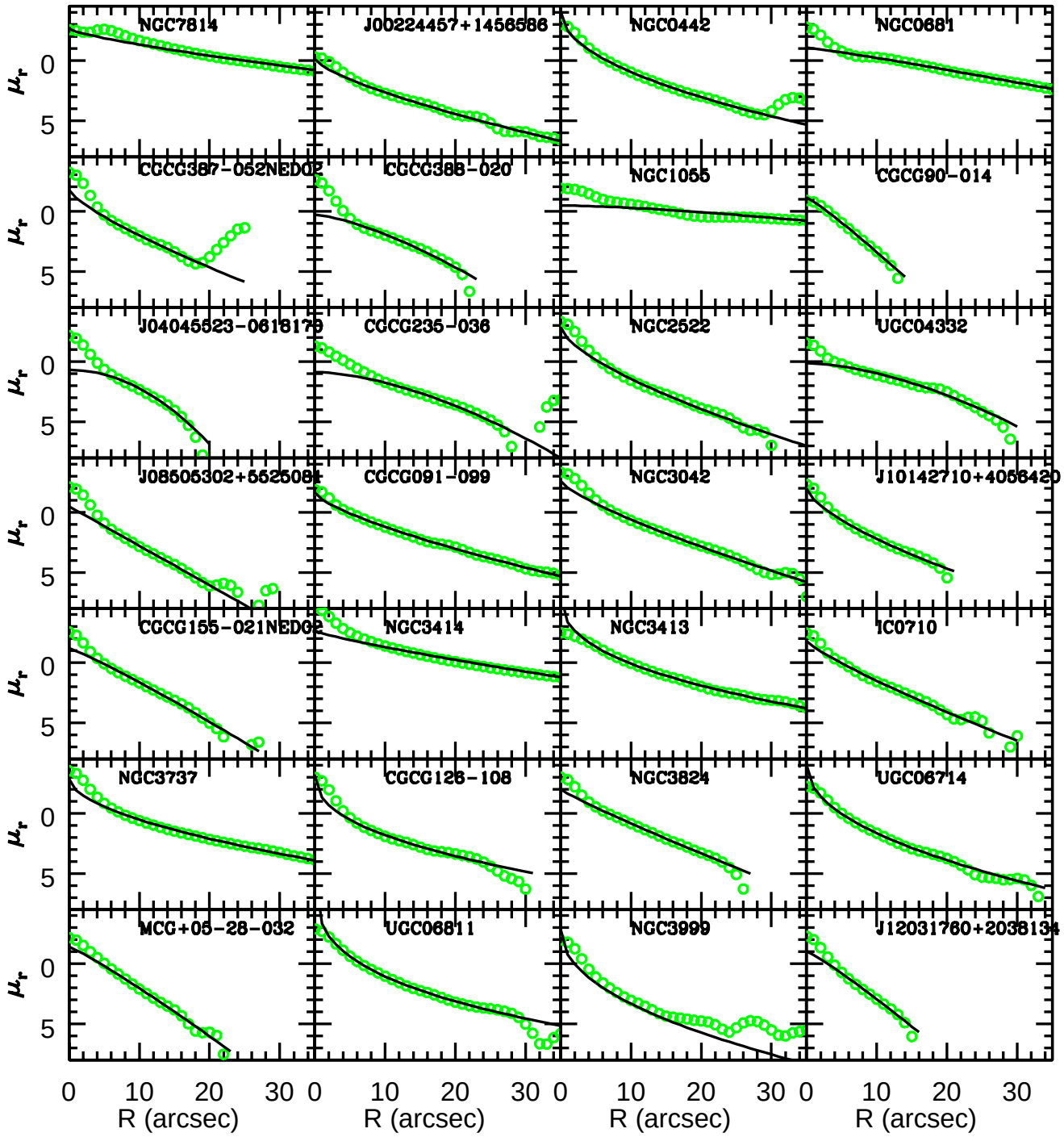

Figure 4. Single component Sérsic function fit to the minor-axis profiles of galaxies that show prominent stellar halos. The circles indicate the data points while the solid lines are the fitting result.

2005; Kim et al. 2006; Janz et al. 2014; Seo & Ann 2018).

Figure 6 shows the frequency distribution of the Sérsic index of prominent stellar halos with (solid lines) and without (dotted lines) the central luminosity excess, respectively. The prominent stellar halos of the sample galaxies with a central luminosity excess have small n, while those without a central luminosity excess show double peaks, with one peak at $n \approx 1.3$ and the other peak at $n \approx 2.8$. There are only two galaxies (4.3%) that have n larger than 2.4 among galaxies with a central luminosity excess, while 63% of galaxies without central luminosity excess have n larger than 2.2. Thus, the extraplanar prominent structure without central luminosity excess can be thought of as the extended bulges.

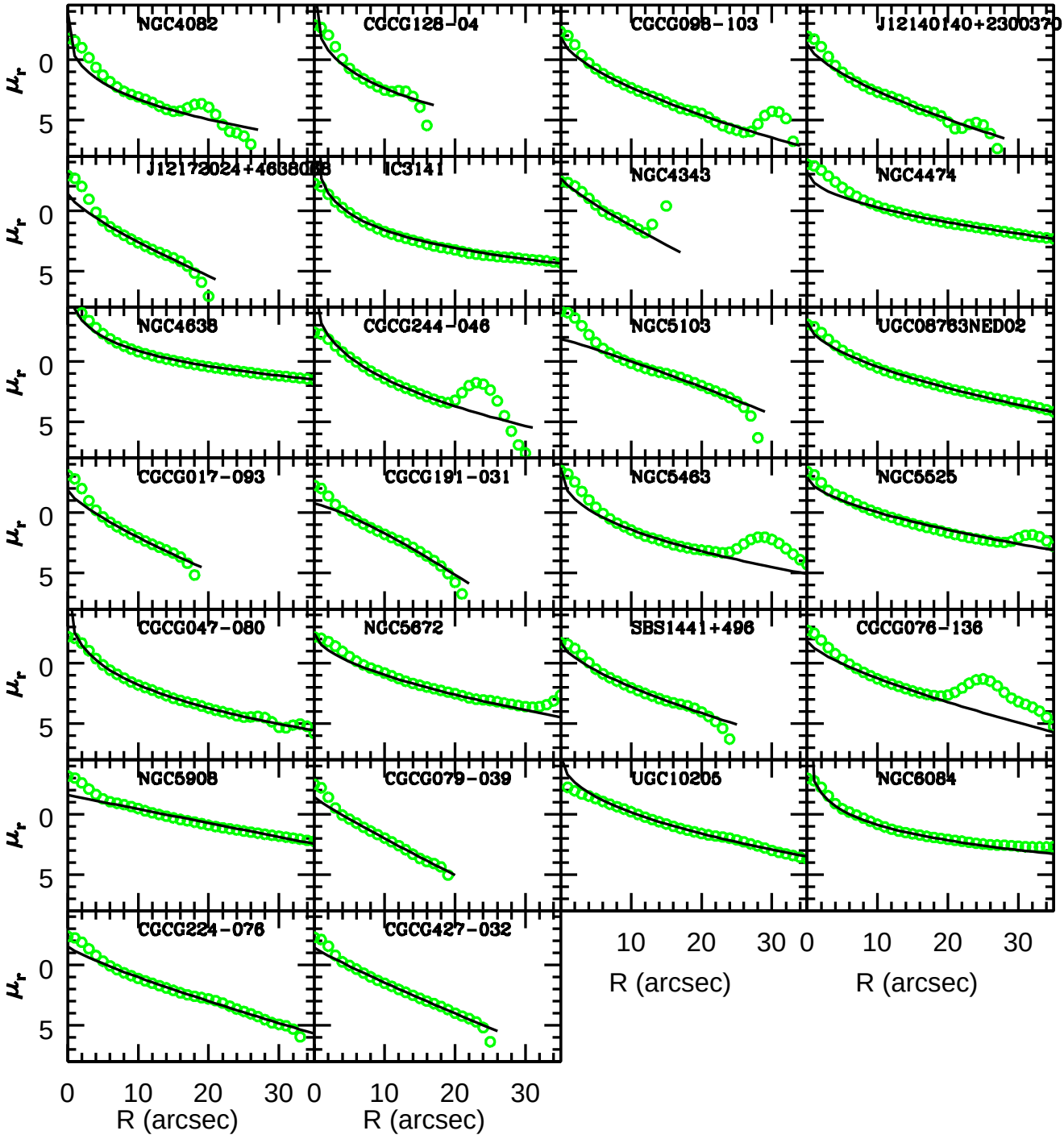

Figure 4. *Continued.*

3.4. Dependence on the Physical Properties of Galaxies

The dependence of the Sérsic index n, derived from the single-component fitting, on the two observable physical parameters, the r-band absolute magnitude (M_r), and the velocity dispersion (σ), are investigated. Both parameters are closely related to the mass of a galaxy, which is a key parameter that controls the formation and evolution of a galaxy (Peng et al. 2012). Figure 7 shows the distribution of n as a function of M_r (lower panel) and σ (upper panel). As shown in the lower panel of Figure 7, there is no clear correlation between the Sérsic index and the luminosity. There may be, however, a tendency of smaller n for less luminous galaxies ($M_r > -20$). More specifically, there are no prominent stellar halos that have n larger than ~ 2 for galaxies with $M_r > -20$, but prominent stellar halos with n larger than ~ 2 are observed in bright galaxies

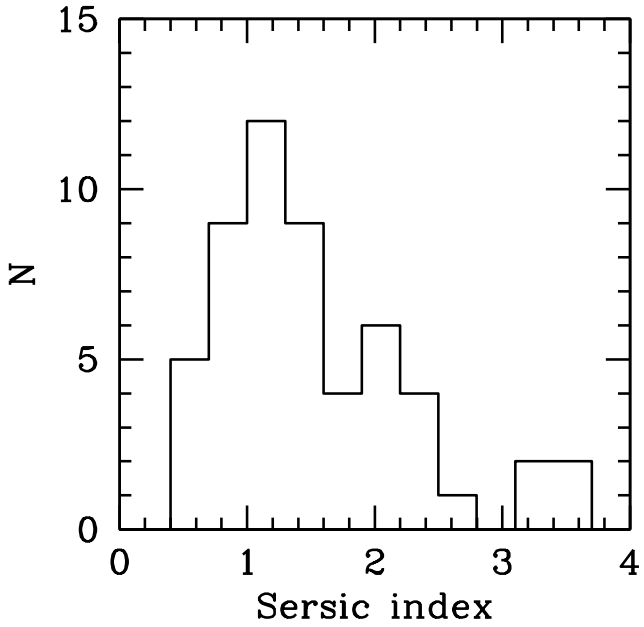

Figure 5. Frequency distribution of the Sérsic index for the single component model.

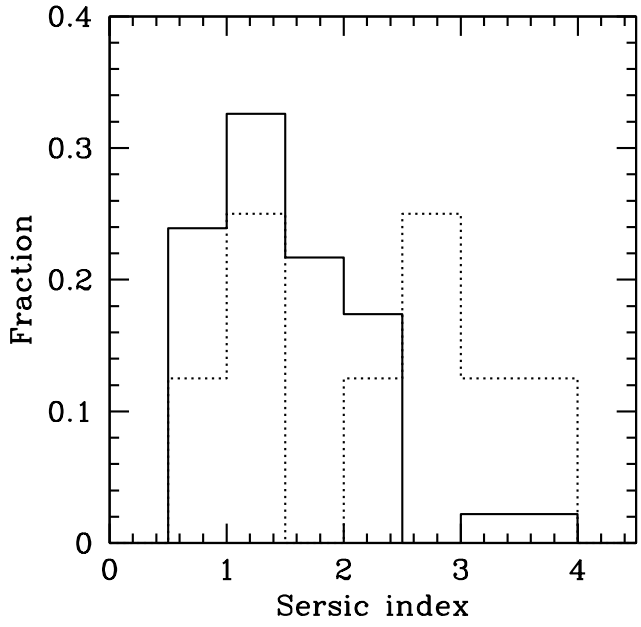

Figure 6. Frequency distribution of the Sérsic index for the single component model grouped by the presence/absence of a central luminosity excess. Galaxies with a central excess are represented by the solid line while those without central excess are plotted by dotted line.

($M_r < -20$). However, even for bright galaxies, their stellar halos are likely to have the Sérsic index of $n \approx 2$.

The upper panel of Figure 7 shows the distribution of n as a function of σ. There is no strong correlation between the two parameters, but there is a tendency of increasing n with increasing σ. It is also apparent that there are no prominent stellar halos that have a large Sérsic index ($n > 2.2$) for galaxies with velocity dispersions less than $\sigma = 150$ km s^{-1}. Thus, the dependence of the Sérsic index on the velocity dispersion is very similar to the dependence of the Sérsic index on the luminosity.

The structure of a galaxy formed through major mergers is different from that formed through a monolithic collapse of galactic proto-clouds. Giant ellipsoidal structures (Sérsic index of $n \approx 4$) are likely to be made by violent mergers, while disks (Sérsic index of $n \approx 1$) are made by dissipational collapse of proto-clouds that have non-negligible angular momentum. The absence of large Sérsic index ($n > 2.2$) for galaxies with $M_r > -20$ or $\sigma < 140$ km $^{-1}$, i.e, relatively low mass galaxies, suggests that major mergers do not play a significant role for less luminous galaxies with prominent stellar halos. It is worth noting that our dividing value of $n = 2.2$ is the same as the critical value suggested by Fisher & Drory (2008) who used this value to divide pseudobulges from classical bulges. If galaxies with small Sérsic indices did not form through major mergers, then the majority of prominent stellar halos must be caused by other mechanisms. This is because $\sim 70\%$ of prominent stellar halos have a Sérsic index less than the critical value, regardless of luminosity or mass.

3.5. Local Background Density

The local background density (Σ) is used to examine the environmental dependence of the Sérsic index. The local background density can be derived using a variety of approaches (Muldrew et al. 2012), but the nth nearest neighbor method with $n = 5$ is used here. The definition of neighbor galaxy by Ann (2017) is used where a neighboring galaxy is defined to have a velocity difference less than the linking velocity $\Delta V = 500$ km s^{-1}, and a luminosity brighter than the limiting magnitude of the volume-limited sample. The background density using the projected distance to the $5th$ nearest galaxy is defined as ,

$$\Sigma_5 = \frac{5}{4\pi r_{p,5}^2},$$

where $r_{p,5}$ is the projected distance to the 5th nearest neighbor galaxy. The local background density is normalized by the mean background density ($\bar{\Sigma_5}$).

Figure 8 shows the histogram of the local background density of the prominent stellar halos along with that of SDSS galaxies with redshift less than $z = 0.04$. There is not much difference between the two distributions. But, the present sample shows somewhat larger fractions at high density regions and smaller fractions at low density regions than the full sample. If we divide the full sample into the blue galaxies and red galaxies, the local background density of the present sample is more similar to that of red galaxies. The low density tail of the present sample is due to the spiral galaxies.

Since there is a tight relationship between the luminosity of a galaxy and the local background density

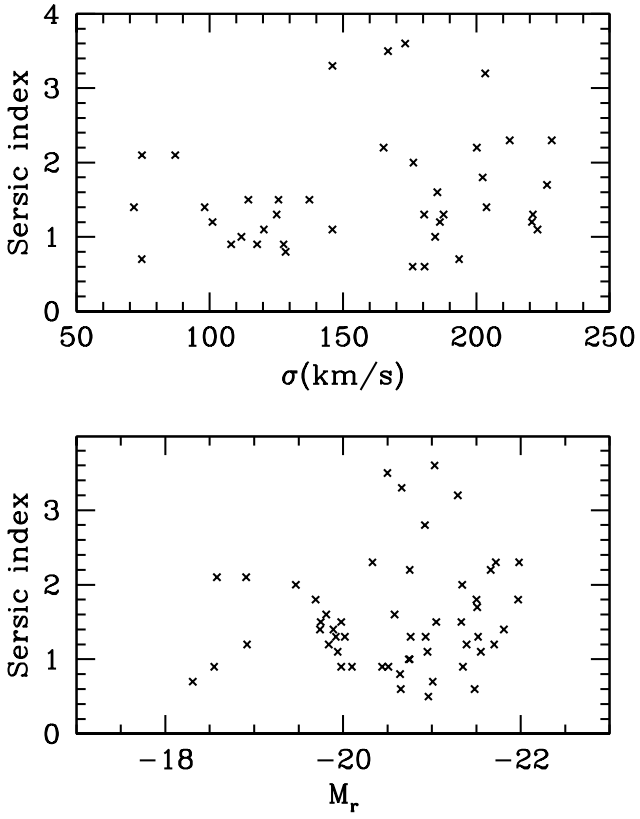

Figure 7. Correlations between physical parameters and the Sérsic index for the single component model. n-σ in the upper panel and n-M_r in the lower panel.

(Goto et al. 2003; Park et al. 2007), we used galaxies brighter than $M_r = -20$ to examine the environmental dependence of the Sérsic index. Fig. 9 shows the frequency distribution of the local background density for prominent stellar halos for galaxies brighter than $M_r = -20$. The distribution of prominent stellar halos with $n < 2.2$ is similar to that of the background galaxy distribution, while the distribution of the prominent stellar halos with $n > 2.2$ shows a much narrower distribution, with maximum frequency at $\Sigma_5/\bar{\Sigma_5} = 0.75$. However, due to the small sample size for the galaxies with large n, this result could be due to statistical noise. We carried out a K-S test and found that there is no significant difference between the two groups. The K-S test gives $p = 0.21$.

4. Discussion and Conclusions

We have analyzed the luminosity profiles along the minor-axis of disk galaxies with luminous halos. Many previous studies considered the prominent stellar halo to be an extended bulge, which is well fitted by the $r^{1/4}$-law (Wainscoat et al. 1990; Emsellem et al. 1996). However, in this study it is treated as a stellar halo which is luminous enough to be observed. The reason for this is that most of the sample galaxies have bright central regions that are assumed to be the central bulge component. They are represented by a central excess of light in the surface brightness profile along the minor-axis when the observed profile is fitted by a single Sérsic

Table 2
Sérsic index of prominent stellar halos.

ID	n	u_{eff} [a]	r_{eff} [b]	n_b	n_h	Σ_5' [c]
354822	1.3	-0.16	1.84	1.0	0.6	-1.470
381062	1.4	2.56	4.82	4.0	1.7	-1.980
2092266	2.0	-0.07	2.39	1.0	0.8	0.142
323194	0.9	0.54	2.15	1.0	0.5	-0.399
1742502	1.3	0.74	2.35	1.0	0.3	-0.138
809401	0.7	1.48	3.96	1.0	0.4	-0.428
1767358	0.7	0.68	2.32	1.0	0.5	-0.255
764571	0.9	0.46	2.19	0.9	0.9	-0.063
326159	0.5	1.41	3.72	1.0	0.4	-1.670
1728488	0.6	1.82	6.58	1.0	0.4	0.040
1905088	1.5	0.08	1.74	1.0	0.7	0.187
1875243	0.6	1.08	3.88	1.0	0.4	0.718
225814	1.0	1.33	3.36	1.0	0.6	1.290
2257869	1.4	1.07	2.64	4.0	1.2	-0.425
78806	1.3	-0.12	1.74	4.0	1.3	-1.030
1248278	1.5	0.93	2.62	1.0	0.9	-0.347
1960169	0.9	0.40	3.77	1.0	0.5	0.579
2204882	1.2	-0.40	1.48	1.0	0.5	-0.015
1894107	2.5	-0.56	0.22	1.0	0.8	-0.143
2221022	1.2	0.44	3.93	1.0	0.5	0.186
965668	1.8	0.71	4.23	4.0	0.9	1.310
2356878	2.3	1.54	3.68	1.0	0.5	0.627
873264	1.1	0.05	2.60	1.0	0.8	-0.658
253847	2.1	0.14	0.86	1.0	0.3	0.007
2205307	0.9	0.19	2.29	1.0	0.2	-0.362
901271	3.2	-0.86	2.03	1.0	0.2	0.790
2322850	2.1	1.39	1.23	1.0	1.4	1.820
2333089	0.9	0.55	1.80	1.0	0.5	0.757
1061991	3.3	2.92	3.92	1.0	0.3	-0.706
2247528	3.5	1.01	2.52	1.0	0.3	0.844
2414948	1.6	1.22	3.50	1.0	1.0	-0.394
2311827	1.5	1.57	3.07	1.0	0.7	-0.167
1202224	1.3	1.10	2.52	1.0	0.5	0.218
2319495	2.2	2.20	2.70	0.2	1.0	-0.001
1288874	1.2	-0.43	0.41	0.2	1.0	1.830
1828259	2.0	0.76	1.47	4.0	1.3	1.120
959348	1.6	2.06	1.49	4.0	10.0	1.060
1176719	2.8	-1.02	1.73	1.0	1.0	0.338
1227719	0.9	-0.26	0.65	1.0	0.4	-0.409
1989264	1.8	0.25	5.30	1.0	0.6	1.740
49109	1.3	0.65	3.30	1.0	0.6	-0.052
1838833	0.8	0.65	3.06	1.0	0.4	-0.547
1340227	2.3	1.01	3.93	0.2	0.4	0.710
2380372	1.7	0.45	4.71	1.0	0.6	-0.358
1348148	3.6	0.14	2.66	1.0	1.0	0.100
1913169	1.8	1.05	2.43	0.2	1.0	-0.064
980767	1.5	1.17	4.17	1.0	0.4	-0.560
1430278	1.4	0.83	5.30	0.2	1.0	0.137
2412381	1.0	0.24	2.66	1.0	0.4	0.450
1423817	1.1	0.62	1.95	1.0	1.2	-0.524
1393362	2.2	-0.51	3.71	1.0	0.4	-0.660
2001255	2.3	3.94	4.12	0.2	1.0	-0.630
532728	1.2	0.71	5.41	1.0	0.6	1.120
726224	1.1	0.58	3.91	1.0	0.8	1.100

[a] Effective surface brightness - μ_{sky}.
[b] Effective radius in unit of arcsec.
[c] Σ_5' is defined as $\log(\Sigma_5/\bar{\Sigma_5})$.

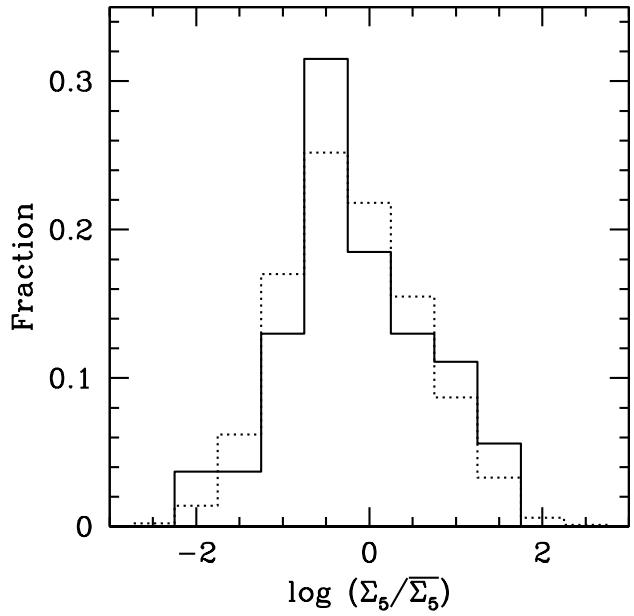

Figure 8. Frequency distribution of the local background density of the prominent stellar halos (solid lines) compared with SDSS galaxies that have redshift less than $z = 0.04$.

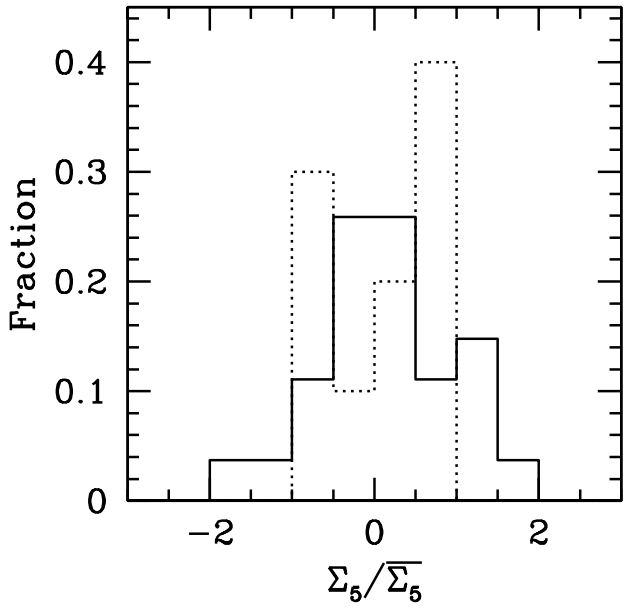

Figure 9. Frequency distribution of the local background density of the prominent stellar halos with $n < 2.2$ (solid lines) compared with the cases for $n > 2.2$. We used galaxies brighter than $M_r = -20$.

profile. The average Sérsic index n of the single component fits is $n = 1.1 \pm 0.9$, and the majority of sample galaxies have n less than ~ 2.2. The small n also supports the assumption that the extended regions are prominent stellar halos rather than extended bulges. In the literature, there are some studies that consider the luminous spheroidal component as a prominent stellar halo (Harris et al. 1984; Burkhead 1986; Wagner et al. 1989) although some authors have not explicitly used the terminology spheroid (Burkhead 1986).

The Sérsic index n of prominent stellar halos is quite different from that of classical bulges. Approximately 80% of prominent stellar halos in the sample have n smaller than the critical value of $n = 2.2$, which divides the bulges of disk galaxies into classical bulges and pseudobulges (Fisher & Drory 2008). Classical bulges have n greater than 2.2, and pseudobulges have n smaller than 2.2. Given that the Sérsic index n is a shape parameter which is closely related to the galaxy formation mechanism, the majority of the stellar halos are formed by mechanisms different from that for the classical bulge formation. Prominent stellar halos do not seem to have formed from major mergers followed by violent relaxation because resulting substructures would have large n. If the luminous spheroidal components are bulges, they are likely to be pseudobulges because of their small n, since pseudobulges are thought to be made through the secular evolution of disk galaxies, driven by non-axisymmetric potential such as a bar (Kormendy & Kennicutt 2004; Okamoto 2013). However, luminous structures around the disks are not considered to be pseudobulges because of their extent which is comparable to the disks. Since pseudobulges are made of disk material, the luminosity of pseudobulges is not expected to dominate over the disk luminosity.

We have examined the dependence of the Sérsic index of prominent stellar halos on the physical properties of galaxies and their environment. The physical properties considered here are the galaxy luminosity (M_r) and the central velocity dispersion (σ). As shown in Figure 7, galaxies with low luminosities ($M_r \gtrsim -20$) or low velocity dispersions ($\sigma \lesssim 150$ km s^{-1}) have Sérsic indices smaller than $n \approx 2.2$, while galaxies with high luminosities and high velocity dispersions have a wide range of Sérsic indices including $n > 2.2$. If a large Sérsic index is considered to be related to the substructures formed through merger induced violent relaxation, then the prominent stellar halos of massive galaxies must have origins different to those of less massive galaxies. One plausible scenario for the origin of the prominent stellar halos that have n smaller than 2.2 is the intensive $in-situ$ star formation. The fact that there is no environmental dependency on the prominent stellar halos supports the above scenario, since supernova explosions are an internal process which does not depend on the environment.

In the ΛCDM cosmology, the stellar halos of disk galaxies are formed by the debris of accreted satellites (Bullock & Johnston 2005; Read et al. 2006; Sales et al. 2007; Font et al. 2008; de Lucia & Helmi 2008; Johnston et al. 2008; Font et al. 2011) as well as $in-situ$ halo stars (Cooper et al. 2015). Halo stars formed $in-situ$ include heated disk stars which are ejected into the halo. These heated disk stars make a negligible contribution to the total halo mass (Cooper et al. 2015), but they contribute significant fractions in the inner halo, simi-

lar to the fraction of stars from satellite debris (Purcell et al. 2010; Font et al. 2011; McCarthy et al. 2011). The disrupted debris of accreted satellites and $in-situ$ halo stars are a good explanation for the faint stellar halos such as that of the Milky Way or M31. However, they can not account for the prominent stellar halos presented in this study, because the luminosity of the prominent stellar halos is brighter than the disk luminosity. Since the present sample of prominent stellar halos is observed in early-type disk galaxies, mostly S0 and S0/a, the cause of prominent stellar halos are thought to be related to the same feedback mechanism that produces lenticular galaxies. The thermal feedback model by Brook et al. (2004) seems to provide a promising mechanism for producing prominent stellar halos, as well as gas poor disks such as those of S0 galaxies. A significant fraction of the stars in prominent stellar halos can be considered to be due to the $in-situ$ star formation from the gas ejected from the disk by violent supernova explosions. It is worth noting that the thermal feedback model in Brook et al. (2004) produces stellar halos similar to those shown in the present study, while their adiabatic feedback model shows stellar halos similar to those of nearby spiral galaxies such as the Milky Way.

ACKNOWLEDGMENTS

We would like to thank the anonymous referee for their suggestions and corrections. We also thank Dong-Kyu Lee for careful reading the manuscript. This work was supported by the NRF Research grant 2015R1D1A1A09057394.

REFERENCES

Abadi, M. G., Navarro, J. F., & Steinmetz, M. 2006, Stars Beyond Galaxies: the Origin of Extended Luminous Haloes around Galaxies, MNRAS, 365, 747

Abazajian, K. N., et al. 2009, The Seventh Data Release of the Sloan Digital Sky Survey, ApJS, 182, 543

Abe, F., Bond, I. A., Carter, B. S., et al. 1999, Observation of the Halo of the Edge-On Galaxy IC 5249, AJ, 118, 261

Ann, H. B. 2017, Morphology of Dwarf Galaxies in Isolated Satellite Systems, JKAS, 50, 111

Ann, H. B., Seo, M., & Ha, D. K. 2015, A Catalog of Visually Classified Galaxies in the Local (z 0.01) Universe, ApJS, 217, 27

Bakos, J., & Trujillo, I. 2012, Deep Surface Brightness Profiles of Spiral Galaxies from SDSS Stripe82: Touching Stellar Halos, arXiv:1204.3082

Bell, E. F., et al. 2008, The Accretion Origin of the Milky Way's Stellar Halo, ApJ, 680, 295

Binggeli, B., & Jerjen, H. 1998, Is the Shape of the Luminosity Profile of Dwarf Elliptical Galaxies an Useful Distance Indicator?, A&Ap, 333, 17

Brook, C. B., Kawata, D., Gibson, B. K., & Flynn, C. 2004, Stellar Halo Constraints on Simulated Late-Type Galaxies, MNRAS, 349, 52

Bullock, J. S., & Johnston, K. V. 2005, Tracing Galaxy Formation with Stellar Halos. I. Methods, ApJ, 635, 931

Burkhead, M. S. 1986, A Photometric Study of M104, AJ, 91, 777

Caon, N., Capaccioli, M., & D Onofrio, M. 1993, On the Shape of the Light Profiles of Early Type Galaxies, MNRAS 265, 1013

Chapman, S. C., Ibata, R., Lewis, G. F., Ferguson, A. M. N., Irwin, M., McConnachie, A., & Tanvir, N. 2006, A Kinematically Selected, Metal-Poor Stellar Halo in the Outskirts of M31, ApJ, 653, 255

Choi, Y.-Y., Han, D.-H., & Kim, S. S. 2010, Korea Institute for Advanced Study Value-Added Galaxy Catalog, JKAS, 43,191

Cooper, A. P., Cole, S., Frenk, C. S., et al. 2010, Galactic Stellar Haloes in the CDM Model, MNRAS, 406, 744

Cooper, A. P., Parry, O. H., Lowing, B., Cole, S., & Frenk, C. S. 2015, Formation of $in-situ$ Stellar Haloes in Milky Way-Mass Galaxies, MNRAS, 454, 3185

Courteau, S., Widrow, L. M., McDonald, M., Guhathakurta, P., Gilbert, K. M., Zhu, Y., Beaton, R. L., & Majewski, S. R. 2011, The Luminosity Profile and Structural Parameters of the Andromeda Galaxy, ApJ, 739, 20

de Jong, R. S., Seth, A. C., Radburn-Smith, D. J., et al. 2007, Stellar Populations across the NGC 4244 Truncated Galactic Disk, ApJ, 667, 49

De Lucia, G., & Helmi, A. 2008, The Galaxy and Its Stellar Halo: Insights on Their Formation from a Hybrid Cosmological Approach, MNRAS, 391, 14

de Vaucouleurs, G. 1958, Photoelectric Photometry of the Andromeda Nebula in the UBV System, ApJ, 128, 465

de Vaucouleurs, G., de Vaucouleurs, A., Corwin, H. G. Jr., Buta, R. J., Paturel, G., & Fouque, P. 1991, Third Reference Catalogue of Bright Galaxies (New York: Springer)

Emsellem, E., Bacon, R., Monnet, G., & Poulain, P. 1996, The Sombrero Galaxy. II. Colours, Kinematics and Line Strengths of the Central Region, A&A, 312, 777

Ferguson, A. M. N., Irwin, M. J., Ibata, R. A., Lewis, G. F., & Tanvir, N. R. 2002, Evidence for Stellar Substructure in the Halo and Outer Disk of M31, AJ, 124, 1452

Fisher, D. B., & Drory, N. 2008, The Structure of Classical Bulges and Pseudobulges: the Link between Pseudobulges and SERSIC Index, AJ, 136, 773

Font, A. S., Johnston, K. V., Bullock, J. S., & Robertson, B. E. 2006, Chemical Abundance Distributions of Galactic Halos and Their Satellite Systems in a DM Universe, ApJ, 638, 585

Font, A. S., Johnston, K. V., Ferguson, A. M. N., Bullock, J. S., Robertson, B. E., Tumlinson, J., & Guhathakurta, P. 2006, The Stellar Content of Galaxy Halos: A Comparison between DM Models and Observations of M31, ApJ, 673, 215

Font, A. S., McCarthy, I. G., Crain, R. A., Theuns, T., Schaye, J., Wiersma, R. P. C., & Dalla V. C. 2011, Cosmological Simulations of the Formation of the Stellar Haloes around Disc Galaxies, MNRAS, 416, 2802

Freeman, K. C. 1970, On the Disks of Spiral and S0 Galaxies, ApJ, 160, 811

Gadotti, D., & Sánchez-Janssem, R. 2012, Surprises in Image Decomposition of Edge-On Galaxies: Does Sombrero Have a (Classical) Bulge? MNRAS, 423, 877

Gilbert, K. M., Font, A. S., Johnston, K. V., & Guhathakurta, P. 2009, The Dominance of Metal-Rich Streams in Stellar Halos: A Comparison Between Substructure in M31 and DM Models, ApJ, 701, 776

Goto, T., Yamauchi, C., Fujita, Y., Okamura, S., Sekiguchi, M., Smail, I., Bernardi, M., & Gomez, P. L. 2003, The

Morphology-Density Relation in the Sloan Digital Sky Survey, MNRAS, 346, 601
Graham, A. W., Trujillo, I., & Caon, N. 2001, Galaxy Light Concentration. I. Index Stability and the Connection with Galaxy Structure, Dynamics, and Supermassive Black Holes, AJ, 122, 1707
Graham, A. W. 2002, The 'Photometric Plane' of Elliptical Galaxies, MNRAS, 334, 859
Grant, N. I., Kuipers, J. A., & Phillipps, S. 2005, Nucleated Dwarf Elliptical Galaxies in the Virgo Cluster, MNRAS, 363, 1019
Harris, W., Harris, H. C., & Harris, G. L. H. 1984, Globular Clusters in Galaxies Beyond the Local Group. III NGC 4594 (the Sombrero), AJ, 89, 216
Helmi A., & White, S. D. M. 1999, Building up the Stellar Halo of the Galaxy, MNRAS, 307, 495
Helmi, A. 2008, The Stellar Halo of the Galaxy, A&ARv, 15, 145
Hes, R., & Peletier, R. F. 1993, The Bulge of M 104 - Stellar Content and Kinematics, A&A, 268, 539
Ho, Luis C., Filippenko, A. V., & Sargent, W. L. W. 1997, A Search for "Dwarf" Seyfert Nuclei. III. Spectroscopic Parameters and Properties of the Host Galaxies, ApJS, 112, 315
Ibata, R., Martin, N. F., Irwin, M., Chapman, S., Ferguson, A. M. N., Lewis, G. F., & McConnachie, A. W. 2007, The Haunted Halos of Andromeda and Triangulum: A Panorama of Galaxy Formation in Action, ApJ, 671, 1591
Ibata, R. A., Ibata, N. G., Lewis, G. F., Martin, N. F., Conn, A., Elahi, P., Arias, V., & Fernando, N. 2014, The Large-Scale Structure of the Halo of the Andromeda Galaxy. I. Global Stellar Density, Morphology and Metallicity Properties, ApJ, 780, 128
Ichikawa, S.-I., Okamura, S., Watanabe, M., Hamabe, M., Aoki, T., & Kodaira, K. 1987, SPIRAL: Surface Photometry Interactive Reduction and Analysis Library, Annals of the Tokyo Astronomical Observatory, 21, 285
Janz, J., Laurikainen, E., Lisker, T., et al. 2014, A Near-Infrared Census of the Multicomponent Stellar Structure of Early-Type Dwarf Galaxies in the Virgo Cluster, ApJ, 786, 105
Jablonka, P., Tafelmeyer, M., Courbin, F., & Ferguson, A. M. N. 2010, Direct Detection of Galaxy Stellar Halos: NGC 3957 as a Test Case, A&A, 513, 78
Jarvis, B. J., & Freeman, K. C. 1985, The Dynamics of Galactic Bulges - NGC 7814 and NGC 4594, ApJ, 295, 324
Johnston, K. V., Hernquist L., & Bolte, M. 1996, Fossil Signatures of Ancient Accretion Events in the Halo, ApJ, 465, 278
Johnston, K. V., Bullock, J. S., Sharma, S., Font, A., Robertson, B. E., & Leitner, S. N. 2008, Tracing Galaxy Formation with Stellar Halos. II. Relating Substructure in Phase and Abundance Space to Accretion Histories, ApJ, 689, 936
Kalirai, J. S., Gilbert, K. M., Guhathakurta, P., Majewski, S. R., Ostheimer, J. C., Rich, R. M., Cooper, M. C., Reitzel, D. B., & Patterson, R. J. 2006, The Metal-Poor Halo of the Andromeda Spiral Galaxy (M31)1, ApJ, 648, 389
Katz, N., & Gunn, J. E. 1991, Dissipational Galaxy Formation. I - Effects of Gasdynamics, ApJ, 377, 365
Kauffmann, G., White, S. D. M., & Guiderdoni, B. 1993, The Formation and Evolution of Galaxies Within Merging Dark Matter Haloes, MNRAS, 264, 201
Kent, S. M. 1988, Dark Matter in Spiral Galaxies. III - The SA Galaxies, AJ, 96, 514
Kim, K. H., Lee, K.-H., & Ann, H. B. 2006, Luminosity Profiles of dE and dS0 Galaxies in the Virgo Cluster, JKAS, 39, 57
Kormendy, J. 1977, Brightness Distributions in Compact and Normal Galaxies. III - Decomposition of Observed Profiles into Spheroid and Disk Components, ApJ, 217, 406
Kormendy, J. 1988, Evidence for a Central Dark Mass in NGC 4594 (the Sombrero Galaxy), ApJ, 335, 40
Kormendy, J., Bender, R., Ajhar, E. A., Dressler, A., Faber, S. M., Gebhardt, K., Grillmair, C., Lauer, T. R., Richstone, D., & Tremaine, S. 1996, Hubble Space Telescope Spectroscopic Evidence for a 1 X 10 9 Msun Black Hole in NGC 4594, ApJ, 473, L91
Kormendy, J., & Kennicutt, R. C. Jr. 2004, Secular Evolution and the Formation of Pseudobulges in Disk Galaxies, ARA&A, 42. 603
Larsen, S. S., Brodie, J. P., Huchra, J. P., Forbes, D. A., & Grillmair, C. J. 2001, Properties of Globular Cluster Systems in Nearby Early-Type Galaxies, AJ, 121, 2974
Lequeux, J., Fort, B., Dantel-Fort, M., Cuillandre, J.-C., & Mellier, Y. 1996, V- and I-Band Observations of the Halo of NGC 5907, A&A, 312, 1
Lequeux, J., Combes, F., Dantel-Fort, M., Cuillandre, J.-C., Fort, B., & Mellier, Y. 1998, NGC 5907 Revisited: a Stellar Halo Formed by Cannibalism?, A&A, 334, 9
McCarthy, I. G., Font, A. S., Crain, R. A., Deason, A. J., Schaye, J., & Theuns, T. 2011, Global Structure and Kinematics of Stellar Haloes in Cosmological Hydrodynamic Simulations, MNRAS, 421, 190
McConnachie, A. W., Chapman, S. C., Ibata, R. A., Ferguson, A. M. N., Irwin, M. J., Lewis, G. F., Tanvir, N. R., & Martin, N. 2006, The Stellar Halo and Outer Disk of M33, ApJ, 647, 25
McQuinn, K. B. W., Skillman, E, D., Dolphin, A. E., Berg, D., & Kennicutt, R. 2016, The Distance to M104, AJ, 152, 144
Mollenhoff, C., & Heidt, J. 2001, Surface Photometry of Spiral Galaxies in NIR: Structural Parameters of Disks and Bulges, A&A, 368, 16
Morrison, H. L., Miller, E. D., Harding, P., Stinebring, D. R., & Boroson, T. A. 1997, AJ, 113, 2061
Mouhcine, M., Rejkuba, M., & Ibata, R. 2007, The Stellar Halo of the Edge-On Galaxy NGC 891, MNRAS, 381, 873
Mould, J. R., et al. 2000, The Hubble Space Telescope Key Project on the Extragalactic Distance Scale. XXVII. A Derivation of the Hubble Constant Using the Fundamental Plane and Dn-lations in Leo I, Virgo, and Fornax, ApJ, 529, 786
Muldrew, S. I., et al. 2012, Measures of Galaxy Environment - I. What Is 'Environment'?, MNRAS, 419, 2670
Okamoto, T. 2013, The Origin of Pseudo-Bulges in Cosmological Simulations of Galaxy Formation, MNRAS 428, 718
Okamura, S. 1988, Surface Photometry of Galaxies, PASP, 100, 524
Park, C., Choi, Y.-Y., Vogeley, M. S., Gott, J. R. III, Blanton, M. R., & SDSS Collaboration, Environmental Dependence of Properties of Galaxies in the Sloan Digital Sky Survey, ApJ, 658, 898
Peng, Y.-J., Lilly, S. J., Renzini, A., & Carollo, M. 2012, Mass and Environment as Drivers of Galaxy Evolution.

II. The Quenching of Satellite Galaxies as the Origin of Environmental Effects, ApJ, 757, 4

Prugniel, P., & Simien, F. 1997, The Fundamental Plane of Early-Type Galaxies: Non-Homology of the Spatial Structure, A&A, 321, 122

Purcell, C. W., Bullock, J. S., & Kazantzidis, S. 2010, Heated Disc Stars in the Stellar Halo, MNRAS, 404, 1711

Read, J. I., Pontzen, A. P., & Viel, M. 2006, On the Formation of Dwarf Galaxies and Stellar Haloes, MNRAS, 371, 885

Romanowsky, A. J., Martinez-Delgado, D., Martin, N. F., Morales, G., Jennings, Z. G., GaBany, R. J., Brodie, J. P., Grebel, E. K., Schedler, J., & Sidonio, M. 2016, Satellite Accretion in Action: A Tidally Disrupting Dwarf Spheroidal around the Nearby Spiral Galaxy NGC 253, MNRAS, 457, L103

Ryden, B. S., Terndrup, D. M., Pogge, R. W., & Lauer, T. R. 1999, Detailed Surface Photometry of Dwarf Elliptical and Dwarf S0 Galaxies in the Virgo Cluster, ApJ, 517, 650

Sackett, P. D., Morrisoni, H. L., Harding, P., & Boroson, T. A. 1944, A Faint Luminous Halo That May Trace the Dark Matter around Spiral Galaxy NGC5907, Nature, 370, 441

Sales, L. V., Navarro, J. F., Abadi, M. G., & Steinmetz, M. 2006, Satellites of Simulated Galaxies: Survival, Merging and Their Relationto the Dark and Stellar Haloes, MNRAS, 379, 1464

Searle, L., & Zinn, R. 1978, Compositions of Halo Clusters and the Formation of the Galactic Halo, ApJ, 225, 357

Seo, M., & Ann, H. B. 2018, in preparation

Sérsic J. L. 1968, Atlas de Galaxias Australes (Cordoba: Observatorio Astronomico)

Seth, A., de Jong, R., Dalcanton, J,, & GHOSTS Team. 2006, Detection of a Stellar Halo in NGC 4244, IAUS, 241, 523

Springel, V., Frenk, C. S., White, S. D. M., & Simon, D. M. 2006, The Large-Scale Structure of the Universe, Nature, 440, 1137

Steinmetz, M., & Muller, E. 1995, The Formation of Disc Galaxies in a Cosmological Context: Structure and Kinematics, MNRAS, 276, 549

Wainscoat, R. J., Hyland, A. R., & Freeman, A. C. 1990, Near-Infrared Surface Photometry of Three Early-Type, Edge-On Spiral Galaxies - NGC 4594, NGC 7123, and NGC 7814, ApJ, 348, 85

Wagner, S. J., Dettmar, R. J., & Bender, R. 1989, Stellar Kinematics of Bulge, Disk and Nucleus in NGC 4594, A& A, 215, 243

White, S. D. M., & Frenk, C. S. 1991, Galaxy Formation through Hierarchical Clustering, ApJ, 379, 52

Zibetti, S., & Ferguson, A. M. N. 2004, A Faint Red Stellar Halo around an Edge-On Disc Galaxy in the Hubble Ultra Deep Field, MNRAS, 352, 6

Zibetti, S., White, S. D. M., & Brinkmann, J. 2004, Haloes around Edge-On Disc Galaxies in the Sloan Digital Sky Survey, MNRAS, 347, 556

Zolotov, A., Willman, B., Brooks, A. M., Governato, F., Brook, C. B., Hogg, D. W., Quinn, T., & Stinson, G. 2009, The Dual Origin of Stellar Halos, ApJ, 702, 1058

Zolotov, A., Willman, B., Brooks, A. M., Governato, F., Hogg, D. W., Shen, S., & Wadsley, J. 2010, The Dual Origin of Stellar Halos. II. Chemical Abundances as Tracers of Formation History, ApJ, 721, 738